Symmetry reduction in group *4mm* photonic crystals

Cheryl M. Anderson and Konstantinos P. Giapis*
Division of Chemistry and Chemical Engineering, California Institute of Technology, Pasadena, California 91125
(Received 10 January 1997; revised manuscript received 29 May 1997)

The size of absolute band gaps in two-dimensional photonic crystals is often limited by band degeneracies at the lattice symmetry points. By reducing the lattice symmetry, these degeneracies can be lifted to increase the size of existing photonic band gaps, or to create new gaps where none existed for the more symmetric structure. Specifically, symmetry reduction by the addition of different diameter rods into the unit cell of two-dimensional square lattices (Laue group $4mm$) is explored. This approach is especially useful in opening absolute band gaps in structures of dielectric rods in air, which are more easily microfabricated than a crystal of air columns in a dielectric background. Symmetry reduction offers a rational approach for exploring and designing new photonic crystal structures. [S0163-1829(97)03736-3]

I. INTRODUCTION

The past decade has witnessed the start of an exciting new field in optoelectronics. The first assertion in 1987 that periodic dielectric structures could be made to possess a photonic band gap[1,2]—a region of the frequency spectrum where propagating modes are forbidden—has captured the imaginations of researchers around the world. A photonic band gap is analogous to an electronic band gap in semiconductors; this analogy bears promise for photonic crystals to impact optical device applications as semiconductors have done for electronics.

Much of the interest surrounding photonic crystals stems from their ability to provide frequency-mode control of light propagating through them. This property gives photonic crystals the potential to greatly improve the efficiency of optoelectronic devices. For example, radiation losses in high-Q resonance cavities can be reduced by embedding the cavity in a photonic crystal.[3] Frequencies that fall within the photonic band gap are exponentially attenuated with no absorption. The use of an entirely dielectric medium also provides an improvement over traditional metallic shielding methods, where high losses reduce their usefulness at optical frequencies. Fine control of frequency propagation may be obtained through the introduction of ''defect'' modes (localized frequency modes) into the gap, which channel emission to one or a few select frequencies.[3–5] Photonic defect modes, most easily formed by blocks of dielectric material inserted into or removed from the photonic crystal, could lead to thresholdless solid-state lasers and more efficient solar cells.

Many three-dimensional[6–8] and two-dimensional[5,9–11] photonic crystals with band gaps in the microwave region have been fabricated. For the most promising applications, however, it is desirable to have photonic gaps at visible to near-infrared (IR) wavelengths. The frequency at which the band gap occurs is directly related to the size of the scattering elements comprising the lattice. Specifically, the size of the features must be of order $\lambda/2$, where λ is the wavelength at which the gap occurs. A photonic crystal with a band gap in the microwave regime has lattice elements a few millimeters in size, but to achieve a band gap in the visible region of the electromagnetic spectrum requires precise fabrication of lattice elements on the order of $\frac{1}{4}\,\mu$m. Though a method for microfabricating three-dimensional (3D) crystals with full photonic band gaps using standard photolithographic and etching techniques has been proposed,[7] fabrication of such small features is exceedingly difficult. Perhaps for this reason attention has been drawn towards two-dimensional (2D) lattice structures, where fabrication requirements are not as stringent. Several groups have successfully fabricated 2D crystals with near-IR band gaps[12–14] and even visible frequency gaps.[15]

Although 3D photonic crystals suggest the most interesting ideas for novel applications, 2D structures could also find several important uses, as a result of their strong *angular* reflectivity properties over a wide frequency band. For example, 2D photonic crystals with absolute band gaps provide a large stop band for use as a feedback mirror in laser diodes,[16] an improvement over traditional (one-dimensional) Bragg reflectors.

The larger a photonic band gap is, the greater the forbidden region of the frequency spectrum. Thus, it is essential to identify and design crystal structures which possess the largest photonic band gaps for a given dielectric contrast ratio. For two different crystals possessing absolute band gaps of equal size, it may be advantageous from a fabrication standpoint to choose the one that has the band gap occurring at the higher nondimensionalized frequency, $\omega a/2\pi c$, where ω is the frequency, a is the lattice constant, and c is the speed of light in vacuum. For a given filling fraction, the feature size scales with a; thus, the crystal with the higher $\omega a/2\pi c$ should be easier to fabricate. But how does one sift through the countless geometrical arrangements to select manufacturable structures with large band gaps in the desired frequency regime? Theoretical calculations are indispensable, albeit a formidable task in view of the numerous structures to model with many variational parameters (e.g., lattice type, filling fraction, shape of filling element). A rational approach towards the design of photonic crystals is needed, rather than brute-force computation.

Photonic crystals are most valuable when they possess an *absolute* band gap, where propagating modes are forbidden regardless of wave polarization. Many crystals possess band gaps for some light polarizations, but these may not overlap to produce an absolute band gap. Often this is a result of band degeneracies at points of high symmetry in the crystal,

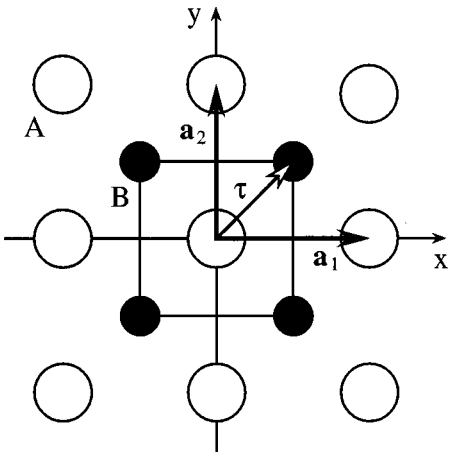

FIG. 1. The two-dimensional single-rod (sites labeled A) and double-rod (sites A and B) square structures, showing the unit cell and the primitive lattice translation vectors.

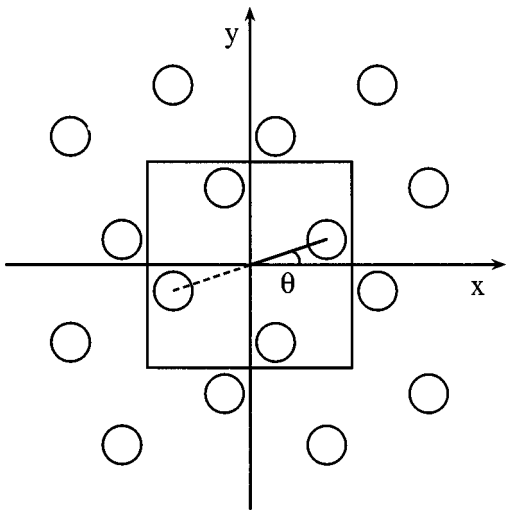

FIG. 2. The two-dimensional glide-symmetry square lattice, with the unit cell indicated. The rod arrangements may be rotated by varying the angle θ to obtain various structures.

which prevent gaps from opening. In some cases the degeneracy can be lifted by reducing the crystal symmetry. Consider for example the 3D face-centered-cubic lattice with spherical dielectric ''atoms,'' which does not possess an absolute photonic band gap.[17] By decreasing the symmetry of the lattice through the introduction of a two-point basis set (which produces the diamond lattice), a degeneracy in the bands is lifted and a full photonic band gap is obtained.[17] In two-dimensional photonic crystals, a similar idea of lattice symmetry reduction has also been effective in producing larger band gaps.[18] Here, we present a more complete description of symmetry reduction in Laue group *4mm* lattices.

II. TWO-DIMENSIONAL SQUARE STRUCTURES

There are three plane groups (two-dimensional space groups) that comprise the square crystal family: *p4*, *p4mm*, and *p4gm*.[19] The first belongs to the Laue group *4*, a relatively low symmetry group that has four symmetry operations. Each of the last two plane groups possesses eight symmetry operations and together they form the Laue group *4mm*. Two-dimensional photonic crystals that have the symmetry of the latter group will be the focus of the present article. Such crystals are formed by circular cross-section rods having a dielectric constant ϵ_a, embedded in a different background material with dielectric constant ϵ_b. The infinitely long rods are assumed to be parallel to the z axis, and the cross section with the x-y plane forms one of the group *4mm* lattices. There are several ways to arrange rods within the unit cell of such a lattice without departing from the symmetry group. The simplest structure (shown by the rods labeled with index A in Fig. 1) contains one rod in each primitive unit cell, with the rod axes arranged on the lattice sites given by the vectors

$$\mathbf{a}(l) = l_1\mathbf{a}_1 + l_2\mathbf{a}_2. \tag{1}$$

Here $\mathbf{a}_1$ and $\mathbf{a}_2$ are primitive lattice vectors and l_1 and l_2 are any two integers, collectively termed l. For the coordinate system shown, the primitive lattice vectors are $\mathbf{a}_1 = a(1,0)$ and $\mathbf{a}_2 = a(0,1)$, where a is the lattice constant. The rods occupying these sites all have diameter d_1.

A different structure can be obtained by the overlay of another square lattice with rods of diameter d_2 on top of the single-rod square lattice, as shown by the index B rods in Fig. 1. The added structure has the same lattice constant a, but is displaced with respect to the first lattice by $\tau = \frac{1}{2}(\mathbf{a}_1 + \mathbf{a}_2)$. This arrangement forms a new lattice when $d_1 \neq d_2$, which is termed the ''double-rod square lattice.'' Both the single-rod and double-rod square lattice structures have the symmetry of the plane group *p4mm*, and all of the rod sites have *4mm* symmetry (i.e., fourfold rotation and mirror planes along the two principal symmetry axes).[19] However, the symmetry is changed slightly in the latter crystal structure, as the smallest unit cell must now contain two rods. In either case, the rods are all assumed to be made of the same dielectric material and are embedded in a different dielectric background. The ratio of the two rod diameters $\beta = d_2/d_1$ can be varied to control the position and size of band gaps. The rod diameter ratio can have values from 0 to ∞, but since β and β^{-1} yield equivalent crystal structures, we examine β values between 0 and 1 only. Note that at either $\beta = 0$ or 1, the single-rod square lattice structure is recovered.

There are several other ways in which one can reduce the symmetry of the single-rod square structure. Consider the ''glide-symmetry square lattice'' as shown in Fig. 2. While at first glance this structure might not appear to be more than a random collection of rods, it belongs in the plane group *p4gm*, thus possessing quite a large number of symmetry operations. Each rod site has $\cdot\cdot m$ symmetry (a mirror plane off the principal axes). The primitive unit cell is shown by the square outline. Varying the angle that the lattice elements form with the primitive unit cell produces a whole class of new structures. We define this angle of tilt, θ, as the angle between the line diagonal of the lattice elements and the x axis, as illustrated in Fig. 2.

New structures can emerge from combining the two previous ideas, i.e., increasing the number of rods in the unit cell and introducing the glide symmetry operation. Consider, for example, the overlay of this new glide-symmetry lattice structure with the single-rod square lattice, such that the rods of the latter lie at the corners and center of the primitive unit

cell. The single-rod square lattice elements have diameter d_1, and the rods associated with the glide lattice have diameter d_2. This complex structure combines two different rod symmetries, with a total of six rods in each primitive unit cell. We will show that even this type of symmetry reduction can yield large absolute band gaps. The glide lattice, superimposed with the single-rod square lattice, gives two parameters that may be varied to maximize the absolute photonic band gap: the ratio of the rod diameters for the two lattices ($\beta = d_2/d_1$) and the tilt angle θ. We examine β values ranging from 0 to ∞, since β and β^{-1} no longer yield equivalent crystal structures. In Fig. 3, three different periodic structures that may be obtained by varying θ are shown. At $\theta = 0°$ [Fig. 3(a)] the structure becomes the double-rod square lattice. We also consider two other lattice positions, as shown in Figs. 3(b) and 3(c) at angles of 18.4° and 45°, respectively.

III. THEORY AND PHOTONIC BAND GAP CALCULATIONS

The propagation of electromagnetic waves through dielectric media is described by Maxwell's equations. These equations can be solved using a plane-wave expansion technique to yield the electromagnetic frequency spectra of waves in a periodic dielectric crystal.[17] To begin, Maxwell's equations are combined to give the wave equation in terms of the magnetic field **H**

$$\nabla \times \left[\frac{1}{\epsilon(\mathbf{x})} \nabla \times \mathbf{H} \right] = \frac{\omega^2}{c^2} \mathbf{H}, \tag{2}$$

where $\epsilon(\mathbf{x})$ is the position-dependent dielectric constant, ω is the frequency, and c is the speed of light in vacuum. The magnetic field $\mathbf{H}(\mathbf{x})$ and the dielectric function $\epsilon(\mathbf{x})$ can be expanded in a sum of plane waves

$$\mathbf{H}(\mathbf{x}) = \sum_{\mathbf{G}} \sum_{\lambda=1,2} h_{\lambda,\mathbf{G}} \hat{\mathbf{e}}_\lambda e^{i(\mathbf{k}+\mathbf{G})\cdot\mathbf{x}}, \tag{3}$$

$$\epsilon(\mathbf{x}) = \sum_{\mathbf{G}} \kappa(\mathbf{G}) e^{i\mathbf{G}\cdot\mathbf{x}}, \tag{4}$$

where $\mathbf{k}$ is the wave vector in the Brillouin zone and $\mathbf{G}$ is a reciprocal-lattice vector. The unit vectors $\hat{\mathbf{e}}_\lambda$ are magnetic wave polarizations orthogonal to $(\mathbf{k}+\mathbf{G})$ and the coefficients $h_{\lambda,\mathbf{G}}$ are the corresponding components of the magnetic field. The Fourier coefficients $\kappa(\mathbf{G})$ are defined in the usual manner by

$$\kappa(\mathbf{G}) = \frac{1}{A_{\text{cell}}} \int_{A_{\text{cell}}} \epsilon(\mathbf{x}) e^{-i(\mathbf{G}\cdot\mathbf{x})} d\mathbf{x} \tag{5}$$

where the integration is carried out over the area A_{cell} of one lattice unit cell.

In two-dimensions, the vectors $\mathbf{k}+\mathbf{G}$ always lie in the plane of the rods. Therefore, the unit vectors $\hat{\mathbf{e}}_1$, $\hat{\mathbf{e}}_2$ must either lie in the plane or along the z axis. This property allows us to rewrite Eq. (2) as two simpler equations, each describing a particular wave polarization. For the magnetic field vector parallel to the axes of the rods (H polarization), $h_{2,\mathbf{k}+\mathbf{G}} = 0$ for all $\mathbf{k}+\mathbf{G}$. Substituting the plane wave expansions into the wave equation gives an eigenvalue problem

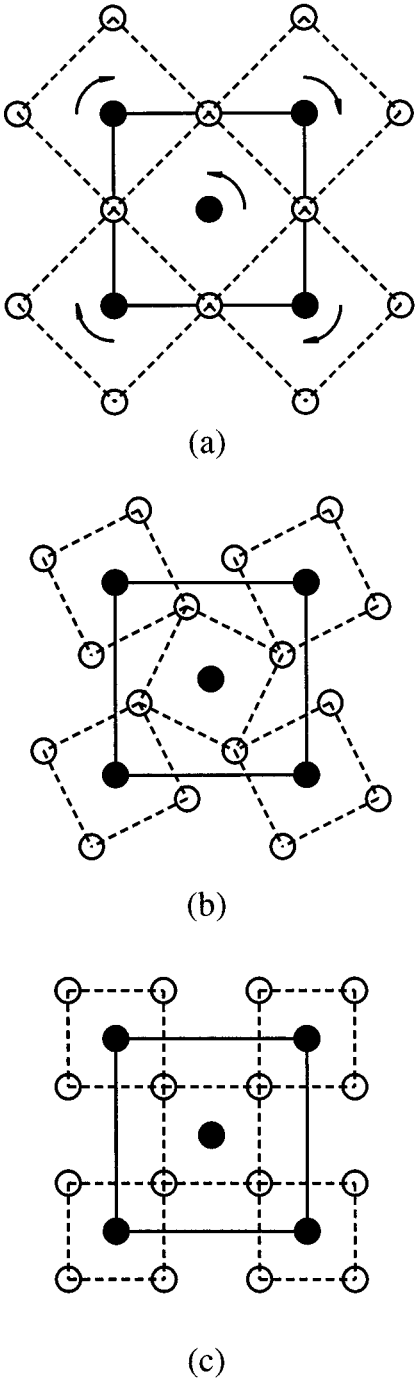

FIG. 3. Two-dimensional square structures produced at tilt angles (a) $\theta = 0°$, (b) $\theta = 18.4°$, and (c) $\theta = 45°$. The arrangement in (a) is the double-rod structure (*p4mm*), shown with a larger unit cell. The arrows in (a) illustrate the direction of rotation—accompanied by lattice compression—that is performed to obtain the glide-symmetry square lattice (group *p4gm*) in (b). Further rotation and compression produces the group *p4mm* structure in (c).

$$\sum_{\mathbf{G}'} (\mathbf{k}+\mathbf{G})\cdot(\mathbf{k}+\mathbf{G}')\,\eta(\mathbf{G}-\mathbf{G}')h_{1,\mathbf{k}+\mathbf{G}'} = \frac{\omega^2}{c^2} h_{1,\mathbf{k}+\mathbf{G}}, \tag{6}$$

where $\eta(\mathbf{G}-\mathbf{G}')$ is a matrix found by inverting the $\kappa(\mathbf{G}-\mathbf{G}')$ matrix of coefficients defined in Eq. (5). By first

expanding the dielectric function $\epsilon(\mathbf{x})$ in a plane wave basis and then inverting the resulting matrix to obtain $\eta(\mathbf{G}-\mathbf{G}')$, faster convergence to the eigenvalues of Eq. (6) is achieved than by direct plane wave expansion of $\epsilon^{-1}(\mathbf{x})$.[20]

For E polarization the electric field vector is parallel to the rod axes and $\mathbf{H}(\mathbf{x})$ is in the rod plane. Here $h_{1,\mathbf{k}+\mathbf{G}}=0$ for all $\mathbf{k}+\mathbf{G}$, yielding another eigenvalue problem:

$$\sum_{\mathbf{G}'} |\mathbf{k}+\mathbf{G}||\mathbf{k}+\mathbf{G}'|\,\eta(\mathbf{G}-\mathbf{G}')h_{2,\mathbf{k}+\mathbf{G}'}=\frac{\omega^2}{c^2}h_{2,\mathbf{k}+\mathbf{G}}. \quad (7)$$

Standard eigenvalue techniques are now used to solve Eqs. (6) and (7) to obtain the propagating wave frequencies for the corresponding polarizations.

In this formulation, all information pertaining to the geometry of the lattice is contained in the coefficient matrix η, or analogously the κ matrix. This provides a very convenient solving routine, as the bulk of the solution ''machinery'' remains in place, while only the κ coefficient matrix changes with different crystal structures.

The integral in Eq. (5) can be expanded and simplified to give

$$\kappa(\mathbf{G})=\begin{cases} f\epsilon_a+(1-f)\epsilon_b, & \mathbf{G}=\mathbf{0}, \\ (\epsilon_a-\epsilon_b)\dfrac{1}{A_{\text{cell}}}\displaystyle\int_{A_{\text{rod}}} e^{-i(\mathbf{G}\cdot\mathbf{x})}d\mathbf{x}, & \mathbf{G}\neq\mathbf{0}. \end{cases} \quad (8)$$

The integral in the second part is now over the rods only. Here, f is the rod filling fraction, defined as $f=A_{\text{rod}}/A_{\text{cell}}$.

For the case of circular cross-section rods of radius r that do not overlap, the coefficients become

$$\kappa(\mathbf{G})=\begin{cases} f\epsilon_a+(1-f)\epsilon_b, & \mathbf{G}=\mathbf{0}, \\ (\epsilon_a-\epsilon_b)\displaystyle\sum_{\mathbf{T}}\frac{2\pi r J_1(Gr)}{A_{\text{cell}}G}e^{-i(\mathbf{G}\cdot\mathbf{T})}, & \mathbf{G}\neq\mathbf{0}, \end{cases} \quad (9)$$

where J_1 is the first order Bessel function of the first kind and $G=|\mathbf{G}|$. The summation is over all rods inside one unit cell with positions described by translation vectors $\mathbf{T}$, measured from the origin of the coordinate axes. For example, consider the glide-symmetry square lattice shown in Fig. 3(b). There are four rods in the unit cell, located at positions described by the translation vectors

$$\mathbf{T}_1=\frac{3}{8}\mathbf{a}_1+\frac{1}{8}\mathbf{a}_2, \quad (10a)$$

$$\mathbf{T}_2=-\frac{1}{8}\mathbf{a}_1+\frac{3}{8}\mathbf{a}_2 \quad (10b)$$

$$\mathbf{T}_3=-\frac{3}{8}\mathbf{a}_1-\frac{1}{8}\mathbf{a}_2, \quad (10c)$$

$$\mathbf{T}_4=\frac{1}{8}\mathbf{a}_1-\frac{3}{8}\mathbf{a}_2. \quad (10d)$$

Substituting these vectors into Eq. (9) and simplifying yields

$$\kappa(\mathbf{G})=\begin{cases} f\epsilon_a+(1-f)\epsilon_b, & \mathbf{G}=\mathbf{0}, \\ (\epsilon_a-\epsilon_b)\dfrac{4\pi r J_1(Gr)}{A_{\text{cell}}G}\left[\cos\left(\dfrac{a}{8}(3g_1+g_2)\right)+\cos\left(\dfrac{a}{8}(g_1-3g_2)\right)\right], & \mathbf{G}\neq\mathbf{0}. \end{cases} \quad (11)$$

Here g_1 and g_2 (integers, denoted collectively by g) are components of the reciprocal lattice vector defined by

$$\mathbf{G}(g)=\frac{2\pi}{a^2}g_1\mathbf{a}_1+\frac{2\pi}{a^2}g_2\mathbf{a}_2. \quad (12)$$

The results that follow were obtained using 729 plane waves for the single-rod square lattice, and 1225 plane waves for the double-rod square lattice and the glide-symmetry square lattice. A greater number of plane waves was required to maintain accuracy for the latter cases due to a more complex unit cell arrangement. The results were tested using 1757 plane waves, for which the band frequencies differed from those calculated with fewer plane waves by a maximum of 0.8%. Most bands differed by less than 0.5%. Thus, we believe that all of the results reported here are accurate to within at least 1% of their true values. The results of the accuracy test also seem to suggest that band calculations with significantly fewer plane waves will not meet the 1% accuracy condition.

IV. PHOTONIC BAND GAP RESULTS

We first examine the single-rod square lattice of air holes in a different dielectric background.[18,21,22] The dispersion relation for a background material with dielectric constant $\epsilon_b=11.4$ (ϵ_{GaAs} at $\lambda\approx 1.5\ \mu$m) and a rod filling fraction of $f=0.77$ is shown in Fig. 4. The figure inset shows the irreducible portion of the Brillouin zone and the corresponding lattice symmetry points. An absolute band gap does exist for this structure, which is produced by an overlap of the H_2 and E_3 band gaps.[23] It is bounded on the lower side by the H-polarization gap boundary, and on its upper side by the E-polarization gap. A summary of our calculations for the single-rod square lattice is shown in the ''gap map'' of Fig. 5, where nondimensionalized frequencies are plotted as a function of the filling fraction. An absolute band gap appears at filling fractions between 0.68–0.79, and has a maximum value of $\Delta\omega=0.0188(2\pi c/a)$ at $f=0.77$.

As the rod filling fraction nears the closed-packed condition ($f=0.785$ for a square lattice of circular rods), the rods in the structure begin to touch and the absolute band gap quickly disappears. The frequency band plot of Fig. 6 for $f=0.8$ demonstrates that the size of the absolute band gap is

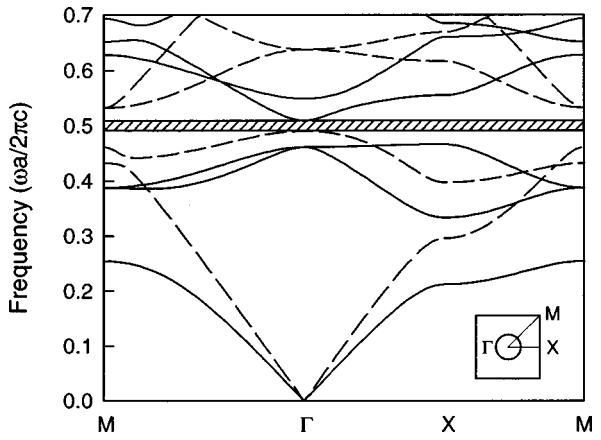

FIG. 4. Frequency band plot for the single-rod square lattice of holes ($f=0.77$) in a background dielectric ($\epsilon_b=11.4$). E-polarization modes are shown by the solid lines, and H-polarization modes by the dashed lines. The H_2 and E_3 gaps overlap to produce an absolute band gap (crosshatched region) of width $0.0188(2\pi c/a)$.

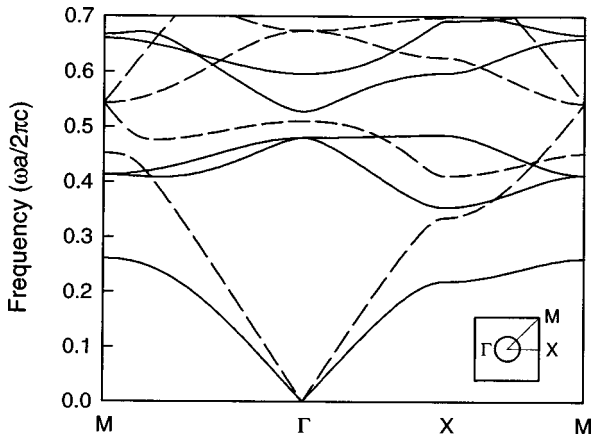

FIG. 6. Frequency band plot for the single-rod square lattice of holes ($f=0.8$) in a background dielectric ($\epsilon_b=11.4$). E-polarization modes are shown by the solid lines, and H-polarization modes by the dashed lines. The absolute band gap disappears at large filling fractions due to an H-polarization band degeneracy at lattice symmetry point **M**.

limited because the second, third, and fourth H-polarization bands are degenerate at the **M** point of the Brillouin zone. If this band degeneracy can be lifted while maintaining (or increasing) the size of the E-polarization gap, a larger absolute band gap will ensue. By placing a smaller diameter rod at the center of each square unit cell (as shown in Fig. 1), the crystal symmetry is reduced. The effect of this symmetry reduction on the square lattice dispersion relation is shown in Fig. 7, where a rod with diameter ratio $\beta=0.16$ has been added to the structure for the same total filling fraction $f=0.8$. The H-polarization degeneracy has been lifted, resulting in a much larger H-polarization gap. Remarkably, the upper E-polarization gap is also greatly enlarged. Thus, the overlap between the two gaps increases, resulting in a much larger absolute band gap. The gap map for the double-rod square lattice when $\beta=0.16$ is shown in Fig. 8. The maximum absolute band gap for the double-rod square structure occurs when $\beta=0.16$ and $f=0.793$. With a gap width of $\Delta\omega=0.0548(2\pi c/a)$, this photonic band gap is nearly *three times* larger than the best value obtained for the single-rod square lattice case.

Extensive calculations have shown that both the filling fraction and the size of the symmetry breaking element are important factors in dictating which crystal arrangements will possess absolute photonic band gaps. In Ref. 24, it was shown that the region of filling fractions where the rods begin to touch or overlap is a critical region of the band gap spectrum, where many band gaps begin to close or open up. Furthermore, it was shown that a connected lattice arrangement was important in the production of H-polarization gaps. The introduction of small rods into the unit cell may work to create larger absolute band gaps by increasing the total rod filling fraction to regimes where large gaps occur, without suffering the consequences of disrupting the lattice connectivity.

Though we have managed to greatly increase the size of

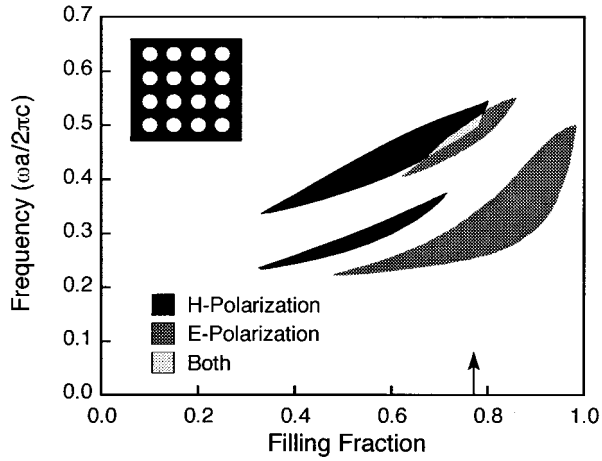

FIG. 5. Gap map for the single-rod square lattice of air holes in a background dielectric ($\epsilon_b=11.4$). An absolute band gap occurs where the upper two polarization gaps overlap. The maximum gap occurs at $f=0.77$ (indicated by the arrow).

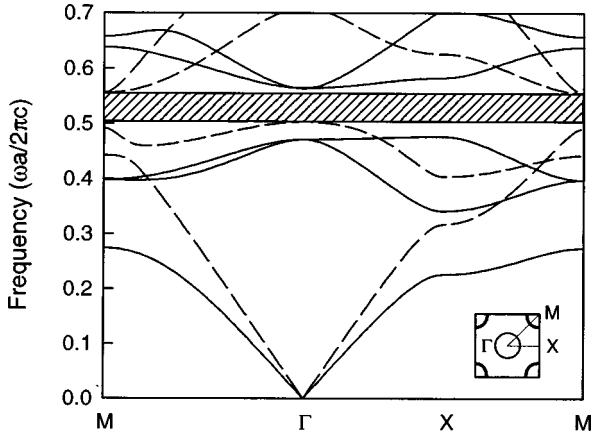

FIG. 7. Frequency band plot for the double-rod square lattice of holes in background dielectric ($\epsilon_b=11.4$), with $f=0.8$ and $\beta=0.16$. Reducing the lattice symmetry by introducing an additional rod into the unit cell lifts the H-polarization (dashed lines) degeneracy while maintaining a large E-polarization (solid lines) gap, resulting in a large absolute band gap (crosshatched region).

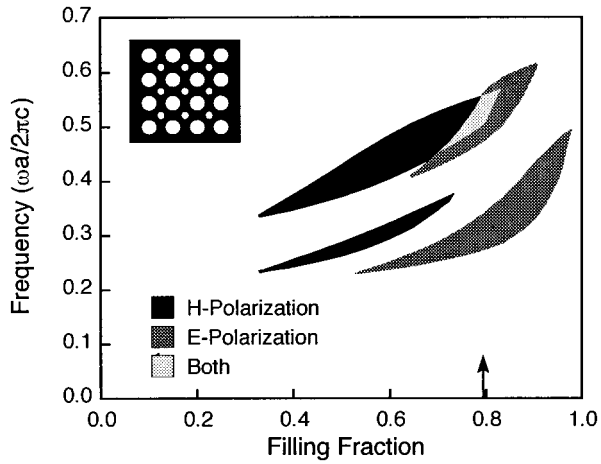

FIG. 8. Gap map for the double-rod square lattice ($\beta=0.16$) of air holes in a background dielectric ($\epsilon_b=11.4$), showing a significantly larger absolute band gap than that for the single-rod lattice. The maximum gap of $0.0548(2\pi c/a)$ occurs at a filling fraction of 0.793 (indicated by the arrow).

the absolute band gap for the square lattice arrangement of holes in dielectric, the resulting structure may not be practical for device applications. The maximum absolute gap condition has a very large filling fraction, $f=0.793$. For a midgap wavelength of 1500 nm (near-IR), the dielectric walls between adjacent holes will be as thin as 6 nm. The precise microfabrication of such small features is extremely difficult. In fact, the results of several studies have shown that to open an absolute photonic band gap in a crystal of air columns in a background dielectric requires the rod filling fraction to always be near the close-packed condition.[9,25–27] Therefore, if we are to identify photonic crystal structures which possess large absolute gaps and can also be easily fabricated, we must consider the opposite arrangement, namely that of dielectric rods in air. It has been shown[26] that for the single-rod square lattice, no absolute gaps occur for the case of dielectric rods in air due to the complete absence of an H-polarization gap. In addition, we have searched all filling fractions of the double-rod square lattice [see Fig. 3(a)] of dielectric rods in air. A modified gap map for a filling fraction of 0.33 is shown in Fig. 9(a), where nondimensionalized frequencies are plotted as a function of the rod diameter ratio β. The band gaps for the single-rod square lattice are obtained when $\beta=0$ or, equivalently, unity.[28] Values of β greater than 1 yield the same structures as those at β^{-1}. The gap map is filled with many large E-polarization gaps that open and close as the rod diameter ratio is varied. The gaps tend to decrease in size at higher frequencies. An interesting feature of this gap map is the presence of ''defectlike'' modes occurring between adjacent E-polarization gaps at high frequencies and low values of β. Three such defect modes are indicated by the horizontal arrows in the figure. In each case, a narrow frequency band appears along the length of a seemingly single E-polarization gap, splitting it in two and creating the isolated mode. From a different perspective, this observation could also be interpreted as follows: the two dissimilar rod sizes in the double-rod square lattice may act as a very regular pattern of defects, creating singular frequency pass bands contained within a band gap. In contrast to the abundance of large E-polarization gaps, only a few small H-polarization gaps exist. The largest H-polarization gaps occur at high frequencies for values of β near 1, but these do not overlap with any E-polarization gaps. The largest absolute gap for the double-rod case was found for a filling fraction of 0.33 and $\beta=0.57$. However, the gap is fairly small, having a maximum width of $\Delta\omega=0.0280(2\pi c/a)$ at a nondimensionalized midgap frequency of 0.752. Thus, other ways must be sought to reduce the symmetry of the square lattice to find arrangements which yield larger absolute band gaps.

The glide-symmetry structure with $\theta=18.4°$, shown in Fig. 3(b), accomplishes a more severe symmetry reduction than that for the double-rod lattice, as mirror planes along major symmetry axes have been eliminated. This symmetry reduction opens several large H-polarization gaps and yields three large absolute band gaps. Band frequency calculations for this structure were performed along the symmetry lines forming the edges of the irreducible 1/8 of the Brillouin zone. The existence of band gaps was confirmed by density of states calculations using uniformly spaced **k** points in the entire first Brillouin zone. The calculations are summarized in the gap map shown in Fig. 9(b) at a filling fraction of 0.33. In this figure, the single-rod lattice is recovered when $\beta=0$. The lowest frequency gap occurs at intermediate values of β, and is entirely limited by the size of the H-polarization gap that opens inside an existing E-polarization gap. This gap is formed by the overlap of H_6 and E_{10} gaps,[23] and has a maximum width of $0.0757(2\pi c/a)$ at $f=0.3$ and $\beta=0.55$. Two other absolute gaps form at and near the equal rod diameter condition. The H-polarization gaps (H_{10} and H_{14}) share one E-polarization gap (E_{18}). The lower frequency gap has a maximum width of $0.0741(2\pi c/a)$ at $f=0.33$ and $\beta=1$, while the upper gap maximum is $0.0762(2\pi c/a)$ at $f=0.33$ and $\beta=1.05$. It is interesting to note that similar gaps do not exist for the double-rod lattice [Fig. 9(a)]. An additional degree of symmetry reduction (accomplished through the introduction of the glide symmetry operation) was necessary to open the new absolute gaps. As all three absolute gaps for the glide-symmetry lattice have similar maximum widths, we can choose which gap to utilize for experimental purposes. From a fabrication standpoint it may be easier to utilize the highest frequency absolute gap. For equal size rods the filling fraction is given by $f=n\pi r^2/a^2$, where n is the number of rods in the unit cell. Therefore, for a given filling fraction the rod radius scales with a, and is inversely proportional to $\sqrt{n}$. With six rods in each glide-symmetry lattice unit cell, it is especially important to make the lattice parameter a as large as possible to increase the smallest feature dimension. However, it has also been shown that higher frequency gaps are more sensitive to random lattice disorder than those at lower frequencies.[29] Since the introduction of a certain amount of disorder during fabrication is probable, especially for small-size features, this may also affect the choice of absolute band gap.

Continuing the study of the symmetry reduction argument, we have also examined the structure shown in Fig. 3(c). The primitive unit cell for this structure contains six rods, as does the previous case, but now the rods line up in diagonal rows ($\theta=45°$). After searching all filling fractions and rod diameter ratios of dielectric rods in air, no absolute

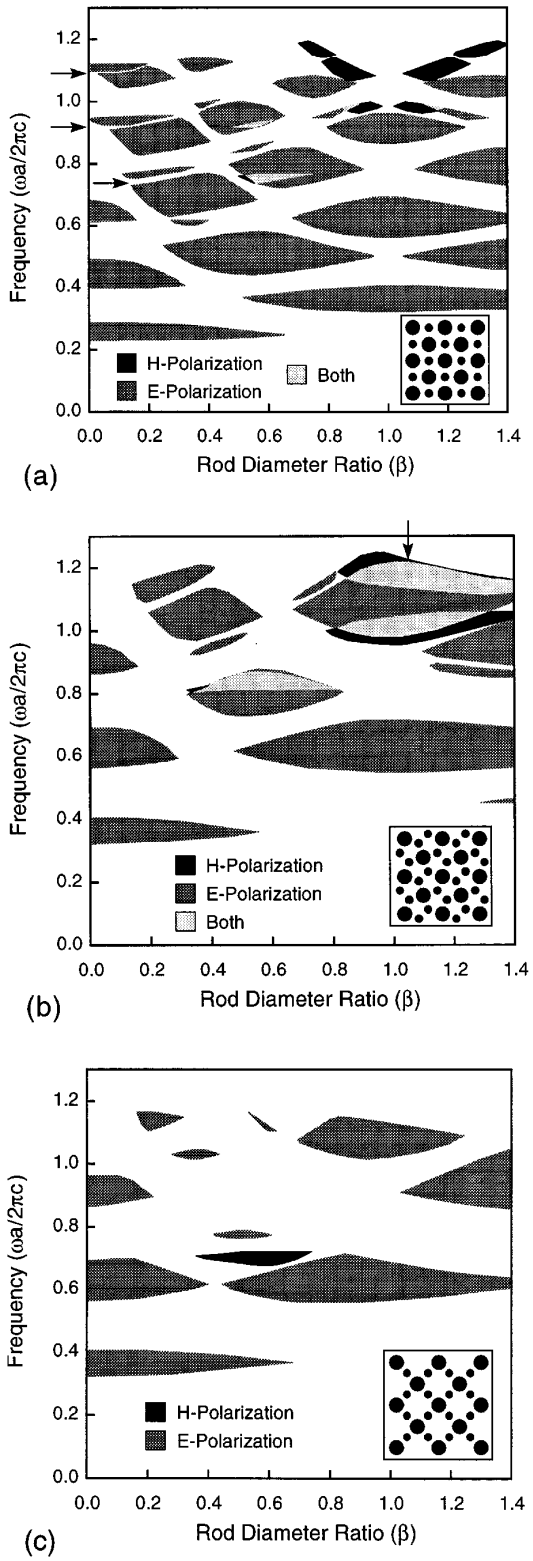

FIG. 9. Gap maps for two-dimensional square structures of dielectric rods ($\epsilon_a = 11.4$) in air produced at tilt angles (a) $\theta = 0°$, (b) $\theta = 18.4°$, and (c) $\theta = 45°$. The lattice filling fraction in each case is $f = 0.33$. The structures in (a) and (c) belong to plane group $p4mm$, and have limited H-polarization gaps. Only the arrangement in (b) possesses the glide symmetry operation (group $p4gm$), which opens several large H-polarization gaps to produce three absolute band gaps. The largest gap (vertical arrow) has a maximum width of $0.0762(2\pi c/a)$ at $\beta = 1.05$. Horizontal arrows in (a) point to defectlike modes present within the E-polarization gaps.

photonic band gaps were found for this structure. A gap map is shown in Fig. 9(c) for a filling fraction of 0.33. Several large E-polarization gaps exist, but only one small H-polarization gap opens up and does not overlap the E-polarization gaps. The lack of absolute gaps makes sense in light of the fact that this crystal structure belongs to the plane group *p4mm*, as do the single-rod and double-rod lattices. All of the *p4mm* symmetry crystals of dielectric rods in air have very small (or absent) H-polarization gaps.

Striking differences may be seen in comparing the three gap maps of Fig. 9. The most symmetric structure, that of Fig. 9(a), possesses the greatest number of large band gaps, albeit for only one polarization. This structure also exhibits defectlike modes in some of the upper E-polarization gaps, a characteristic not seen in the other lattices studied here. It is easy to create E-polarization gaps in ordered crystals comprising of dielectric rods in air. These gaps are usually quite large and robust with respect to changes in the crystal structure.[29] The challenge is to force H-polarization gaps to open at frequencies that overlap with the E-polarization gaps. Introduction of the glide-symmetry operation in Fig. 9(b) has succeeded in this more difficult task, opening three large H-polarization gaps. Some of the E-polarization gaps—present in the more symmetric case—have been eliminated by this reduction in lattice symmetry, but several large gaps survive to create absolute band gaps. In Fig. 9(c), ordered rows of rods are separated with pockets of empty space. The hardy E-polarization gaps remain, though only one small H-polarization gap exists. The remarkable evolution of gaps occurs simply by changing the tilt angle θ.

Our analysis suggests that the best *4mm*-group-based structure for obtaining large absolute band gaps with dielectric columns in air is the structure with glide symmetry, shown in Fig. 3(b). Removing the mirror plane symmetries along the principal axes of the square lattice (present in the $p4mm$ plane group but not in *p4gm*) contributes to the opening of H-polarization gaps, and ultimately produces large absolute band gaps. At first glance, it might seem unlikely that the glide structure would have any gaps at all. However, there are many symmetry operations present within this structure, which apparently are enough to allow gaps to open. This example illustrates the power of the symmetry-reduction idea—it provides a rational way to identify new structures with absolute band gaps that might have otherwise been overlooked. Indeed, it is doubtful as to whether the structure of Fig. 3(b) would have been studied without this motivation.

V. DISCUSSION

Though we have explored a method for systematically identifying new photonic crystal structures, we have not yet detailed a quantitative connection between the degree of symmetry reduction and the size of the absolute photonic gap. Such a relationship—if it exists—would be immensely beneficial for the design of photonic crystals. Other researchers have also searched for the link between crystal properties and band gap opening in an attempt to explain and predict the occurrence of photonic band gaps. Joannopoulos *et al.*,[26] studied electromagnetic fields and lattice connectivity to understand photonic gap openings. Cassagne *et al.*,[27] have in-

vestigated the opening of gaps for 2D hexagonal structures using a perturbative approach. Although these investigations shed light into how gap opening occurs, they also fall short of providing physical rules for selecting the optimal structure. Ideally, deciphering the connection between symmetry reduction and band overlap should enable one to determine the crystal arrangement that yields the maximum absolute band gap for a given dielectric contrast. For the single-rod square lattice, we have seen that band degeneracies at a high symmetry point in the crystal can be lifted by reducing the lattice symmetry. However, we lack an *a priori* understanding as to what ''degree'' the symmetry should be broken to maximize the photonic gaps. Photonic crystal modeling is analogous in many ways to electronic crystal modeling. Though several methods exist for calculating properties of crystals of atoms, these methods do not allow one to exactly determine the ideal structure to optimize a given property (e.g., hardness). Instead, one must first propose a structure and then calculate its crystal properties to determine if the goal has been met. However, judicious guesses of promising structures greatly assist in the study of these materials. In photonic crystal modeling, symmetry reduction can, at the least, be considered as a guiding principle to the design of new photonic structures.

VI. SUMMARY AND CONCLUSIONS

We have shown that the size of absolute photonic band gaps in two-dimensional square lattices can be significantly increased by reducing the lattice symmetry. Specifically, two interpenetrating square lattices with different diameter rods can yield photonic crystals with gaps significantly larger as compared to the single-rod lattice with the same dielectric contrast. For air holes in a background medium of GaAs ($\epsilon = 11.4$), the maximum gap size of the double-rod square lattice was nearly three times the size of the best single-rod lattice band gap at the same dielectric contrast. However, absolute band gaps for crystals of air rods in background dielectric occur at high filling fractions, resulting in thin-walled structures that are difficult to fabricate. This problem may be avoided by fabricating photonic crystals of dielectric rods in air. However, no photonic band gaps exist for either the single-rod or double-rod lattices of dielectric rods in air. By removing the mirror planes of the single-rod lattice geometry through the introduction of the glide symmetry operation, crystals with large absolute band gaps have been obtained. These band gaps occur at moderate filling fractions (≈ 0.35) and thus should be easier to fabricate than those of holes in dielectric. Lattice symmetry reduction provides a guiding principle towards a more rational design of 2D photonic crystals, and might also be successfully applied for band gap engineering in 3D photonic crystals.

ACKNOWLEDGMENTS

Most of the computations were performed on an IBM RS/6000 Workstation awarded through the IBM University Grants Program. The authors are grateful to J. A. Kornfield for allowing free use of her group's workstations. The work of K.P.G. was supported by the Camille and Henry Dreyfus Foundation.

*Author to whom correspondence should be addressed.

[1] E. Yablonovitch, Phys. Rev. Lett. **58**, 2059 (1987).
[2] S. John, Phys. Rev. Lett. **58**, 2486 (1987).
[3] R. D. Meade, K. D. Brommer, A. M. Rappe, and J. D. Joannopoulos, Phys. Rev. B **44**, 13 772 (1991).
[4] E. Yablonovitch *et al.*, Phys. Rev. Lett. **67**, 3380 (1991).
[5] S. L. McCall *et al.*, Phys. Rev. Lett. **67**, 2017 (1991).
[6] E. Yablonovitch and T. Gmitter, Phys. Rev. Lett. **63**, 1950 (1989).
[7] E. Yablonovitch, T. Gmitter, and K. M. Leung, Phys. Rev. Lett. **67**, 2295 (1991).
[8] E. Özbay *et al.*, Phys. Rev. B **50**, 1945 (1994).
[9] R. D. Meade, K. D. Brommer, A. M. Rappe, and J. D. Joannopoulos, Appl. Phys. Lett. **61**, 495 (1992).
[10] W. M. Robertson *et al.*, Phys. Rev. Lett. **68**, 2023 (1992).
[11] S. Y. Lin *et al.*, J. Mod. Opt. **41**, 385 (1994).
[12] T. F. Krauss *et al.*, Nature (London) **383**, 699 (1996).
[13] U. Grüning *et al.*, Appl. Phys. Lett. **68**, 747 (1996).
[14] K. Inoue *et al.*, Phys. Rev. B **53**, 1010 (1996).
[15] H.-B. Lin *et al.*, Appl. Phys. Lett. **68**, 2927 (1996).
[16] D. L. Bullock *et al.*, J. Opt. Soc. Am. B **10**, 399 (1993).
[17] K. M. Ho *et al.*, Phys. Rev. Lett. **65**, 3152 (1990).
[18] C. M. Anderson and K. P. Giapis, Phys. Rev. Lett. **77**, 2949 (1996).
[19] *International Tables for Crystallography*, edited by T. Hahn (Reidel, Boston, 1987).
[20] P. R. Villeneuve and M. Piché, J. Mod. Opt. **41**, 241 (1994).
[21] M. Plihal *et al.*, Opt. Commun. **80**, 199 (1991).
[22] P. R. Villeneuve and M. Piché, Phys. Rev. B **46**, 4973 (1992).
[23] A gap for a particular polarization bounded by the nth and $(n+1)$th frequency bands is designated with subscript n.
[24] J. N. Winn *et al.*, J. Mod. Opt. **41**, 257 (1994).
[25] P. R. Villeneuve and M. Piché, Phys. Rev. B **46**, 4969 (1992).
[26] J. D. Joannopoulos *et al.*, *Photonic Crystals* (Princeton University Press, Princeton, 1995).
[27] D. Cassagne *et al.*, Phys. Rev. B **53**, 7134 (1996).
[28] When $\beta = 1$, the gap positions are shifted by a factor of $\sqrt{2}$ as a result of the change in the unit cell size.
[29] M. M. Sigalas *et al.*, Phys. Rev. B **53**, 8340 (1996).